



UDC 621.762

<https://doi.org/10.17073/1997-308X-2023-1-49-62>

Research article

Научная статья



Microstructure and phase composition of hard alloys produced from nanocrystalline powder mixture WC–6wt.%Co with C, Al and ZrC additives

S. V. Briakunov^{1, 2}, A. S. Kurlov¹ ¹ Institute of Solid State Chemistry of the Ural Branch of the Russian Academy of Sciences
91 Pervomaiskaya Str., Ekaterinburg 620990, Russian Federation² Ural Federal University named after the first President of Russia B. N. Yeltsin
19 Mira Str., Ekaterinburg 620002, Russian Federation kurlov@ihim.uran.ru

Abstract. A large specific surface area of WC nanopowder determines its high chemical activity and makes it very sensitive to various impurities, among which oxygen is most harmful and unavoidable. During heating, oxygen interacts with carbon of WC being removed in the form of CO/CO₂, which finally leads to the appearance of embrittling η-phases in the hard alloy, abnormal growth of WC grains, and formation of a porous microstructure. To prevent heavy decarburization of WC during vacuum sintering of hard alloy from a nanocrystalline powder mixture WC–6wt.%Co, in this work we compared three methods: addition of extra carbon to compensate for carbon loss as a result of decarburization; addition of Al to bind impurity oxygen into Al₂O₃ before it interacts with carbon of WC; and addition of ZrC to compensate for carbon loss and bind impurity oxygen into ZrO₂. Nanocrystalline powder mixtures based on WC–6 wt.%Co with and without additions of C, Al, and ZrC were prepared from microcrystalline powders of WC, Co, Al, ZrC, and carbon black by high-energy milling, then they were compacted in a cylindrical mold by uniaxial pressing at a pressure of ~460 MPa and sintered in graphite crucibles for 15 min at 1380 °C in vacuum of ~10^{–2} Pa. The heating rate to the temperature of sintering was 10 °C/min. The initial powders, powder mixtures prepared therefrom, and sintered hard alloys were certified using X-ray diffraction, chemical analysis, scanning electron microscopy, BET adsorption method, helium pycnometry, and Vickers method. The studies performed showed that the average particle size in all the prepared powder mixtures does not exceed 100 nm, and the content of impurity oxygen in them varies from 3.3 to 4.3 wt.% depending on the additives. It was established that only a part of oxygen contained in the powder mixtures is in the chemisorbed state and takes part in the decarburization of WC during vacuum sintering. The Al additive is completely oxidized during milling of the powder mixture and transforms into nanocrystalline Al₂O₃, which only aggravates carbon loss during sintering and results in the formation of a multiphase and relatively porous microstructure of the hard alloy. On the contrary, using carbon and ZrC additives we managed to prevent the decarburization of WC during sintering of the hard alloy and to form a less porous microstructure in it. It was shown that the presence of ZrO₂ inclusions does not impede intensive growth of WC grains during sintering, but rather promotes it. Carbon deficit slightly suppresses intensive WC grain growth during sintering of hard alloy leading to the formation of η-phases and to an increase in the density and microhardness, but the presence of oxide inclusions Al₂O₃ and ZrO₂ in the microstructure reduces the values of these properties.


Keywords: tungsten carbide, aluminum, zirconium carbide, high-energy milling, nanocrystalline powder, vacuum sintering, decarburization, hard alloy, microstructure, microhardness

Acknowledgements: the study was carried out within the framework of the state assignment of the Institute of Solid State Chemistry of the Ural Branch of the Russian Academy of Sciences No. AAAA-A19-119031890029-7.

The authors kindly acknowledge the assistance of O.V. Makarova in the density measurements and of L.Yu. Buldakova and D.A. Danilov in the determination of carbon and oxygen content in powders.

For citation: Briakunov S.V., Kurlov A.S. Microstructure and phase composition of hard alloys produced from nanocrystalline powder mixture WC–6 wt.% Co with C, Al, and ZrC additives. *Powder Metallurgy and Functional Coatings*. 2023;17(1): 49–62. <https://doi.org/10.17073/1997-308X-2023-1-49-62>

Микроструктура и фазовый состав твердых сплавов, изготовленных из нанокристаллической порошковой смеси WC–6мас.%Co с добавками C, Al и ZrC

С. В. Брякунов^{1,2}, А. С. Курлов¹ 

¹ Институт химии твердого тела Уральского отделения РАН
Россия, 620990, г. Екатеринбург, ул. Первомайская, 91

² Уральский федеральный университет им. первого Президента России Б.Н. Ельцина
Россия, 620002, г. Екатеринбург, ул. Мира, 19

 kurlov@ihim.uran.ru

Аннотация. Большая удельная поверхность нанопорошка WC обуславливает его высокую химическую активность и делает его очень чувствительным к различным примесям, среди которых кислород является наиболее вредной и неизбежной. При нагреве кислород взаимодействует с углеродом WC, удаляясь в виде CO/CO₂, что в конечном итоге приводит к образованию в твердом сплаве охрупчивающих η-фаз, аномальному росту зерен WC и формированию пористой микроструктуры. Для предотвращения сильного обезуглероживания WC при вакуумном спекании твердого сплава из нанокристаллической порошковой смеси WC–6мас.%Co в данной работе сравнивались три способа: добавление избыточного углерода для компенсации потерь в результате обезуглероживания; введение в порошковую смесь алюминия для связывания примесного кислорода в Al₂O₃ до взаимодействия его с углеродом WC; использование добавки ZrC для компенсации потери углерода и связывания примесного кислорода в ZrO₂. Нанокристаллические порошковые смеси на основе WC–6мас.%Co с добавками C, Al, ZrC и без них готовились из микрокристаллических порошков WC, Co, Al, ZrC и сажи с помощью высокоэнергетического размолла, затем компактировались в цилиндрической пресс-форме путем одноосного прессования при давлении ~460 МПа и спекались в графитовых тиглях в течение 15 мин при температуре 1380 °C в вакууме ~10⁻² Па. Скорость нагрева до температуры спекания составляла 10 °C/мин. Аттестация исходных порошков, приготовленных из них порошковых смесей, а также спеченных твердых сплавов осуществлялась с помощью рентгеновской дифракции, химического анализа, сканирующей электронной микроскопии, адсорбционного метода БЭТ, гелиевой пикнометрии и метода Виккерса. Исследования показали, что средний размер частиц во всех приготовленных порошковых смесях не превышает 100 нм, а содержание примесного кислорода в них варьируется от 3,3 до 4,3 мас. % в зависимости от добавок. Установлено, что лишь часть содержащегося в порошковых смесях кислорода находится в хемосорбированном состоянии и принимает участие в обезуглероживании WC при вакуумном спекании. Добавка Al при размоле порошковой смеси полностью окисляется и превращается в нанокристаллический оксид Al₂O₃, что только усугубляет потерю углерода при спекании и приводит к формированию многофазной и относительно пористой микроструктуры твердого сплава. Наоборот, с помощью добавок углерода и ZrC удается предотвратить обезуглероживание WC при спекании твердого сплава и сформировать в нем наименее пористую микроструктуру. Показано, что наличие оксидных включений ZrO₂ не препятствует интенсивному росту зерен WC при спекании, а скорее, наоборот, способствует этому. Дефицит углерода немного сдерживает интенсивный рост зерен WC при спекании твердого сплава, приводя к образованию η-фаз и повышению плотности и микротвердости, но присутствие оксидных включений Al₂O₃ и ZrO₂ в микроструктуре снижает величины этих свойств.

Ключевые слова: карбид вольфрама, алюминий, карбид циркония, высокоэнергетический размол, нанокристаллический порошок, вакуумное спекание, обезуглероживание, твердый сплав, микроструктура, микротвердость

Благодарности: исследование выполнено в рамках государственного задания ИХТТ Уральского отделения РАН № АААА-А19-119031890029-7.

Авторы благодарны О.В. Макаровой за помощь в измерении плотности, а также Л.Ю. Булдаковой и Д.А. Данилову за помощь в определении содержания углерода и кислорода в порошках.

Для цитирования: Брякунов С.В., Курлов А.С. Микроструктура и фазовый состав твердых сплавов, изготовленных из нанокристаллической порошковой смеси WC–6мас.%Co с добавками C, Al и ZrC. *Известия вузов. Порошковая металлургия и функциональные покрытия.* 2023;17(1):49–62. <https://doi.org/10.17073/1997-308X-2023-1-49-62>

Introduction

Thanks to an outstanding combination of high hardness values and impact toughness, hard alloys, compared to other cutting materials (such as diamond or high speed steels), have a wide range of applications in many industries, e.g. as cutting tools (turning, milling, drilling tools) for metalworking, as part of the components of drill bits for well drilling, tunneling, and road pavement removal, as wear-resistant parts in drawing and stamping tools, etc. [1–3].

In the vast variety of available hard alloys, WC–Co system alloys are among the most common and required. The combination of the high hardness and strength of WC, which is maintained even at relatively high temperatures, with the ductility and high impact toughness of Co results in WC–Co alloys with high hardness, strength and wear resistance [4; 5]. Research into the physical, mechanical and performance properties of these alloys continues to this day. In the last three decades, the main efforts were aimed at developing various methods of obtaining nanocrystalline WC powders and mixtures based on them [6–10], as well as methods of their consolidation [11–20] for the production of hard alloys with a submicro- and nanocrystalline structure, which would enable significant improvement of their mechanical properties [21–23].

However, the transition from the use of microcrystalline to nanocrystalline carbide powders also exacerbates their contamination problem. The extremely large specific surface area of nanopowders determines their high chemical activity and makes them very sensitive to various impurities. The surface of carbide nanoparticles may contain adsorbed water and other impurities. Oxygen is the most harmful and unavoidable of these contaminants, its content usually greatly exceeding the total amount of all other impurities and determining the overall purity of the carbide nanopowder [24]. It was shown in [25; 26] that vacuum heating of nanocrystalline WC powders, regardless of their production method, is accompanied by decarburization of WC and leads to a change in their phase composition. When carbon is added to WC nanopowder, the latter retains its single-phase nature, but the strong growth of carbide particles is provoked, transforming the powder into a microcrystalline one. In the case of WC–Co hard alloys produced from nanopowders, decarburization during sintering caused by oxygen adsorbed on the surface of nanoparticles ultimately leads to the formation of embrittling η -phases in the alloy and abnormal growth of carbide grains [27–29].

The study of micro- and nanocrystalline TaC powders has shown that the content of adsorbed oxygen in them increases linearly with the specific surface area of the powder and that most of the oxygen in the

powders is predominantly in the chemisorbed state, forming several monolayers of the Ta₂O₅ oxide phase on the particle surface [30]. An assessment of the possible loss of carbide carbon due to the desorption of chemisorbed oxygen in the form of CO showed that high-temperature sintering of nanocrystalline TaC powders, in contrast to microcrystalline ones, can be accompanied by their significant decarburization, which ultimately leads not only to a change in the composition (y) of TaC _{y} carbide, but also to a change in the phase composition of the entire powder, which was later confirmed experimentally [31]. Besides, the desorption of chemisorbed oxygen in the form of CO and CO₂ during sintering of dense compacts of carbide nanopowders results in the formation of a porous structure [32]. To avoid this, the impurity oxygen must be bound during sintering into strong, hard and refractory oxides that take the place of possible pores before the oxygen begins to interact with the carbon of the carbide. Candidates for this role may be Al or Zr, which have a higher affinity for oxygen compared to W and form the oxides Al₂O₃ and ZrO₂ that are well known as the basis of modern ceramic materials with high mechanical strength, hardness, wear resistance, refractoriness, chemical and corrosion resistance [33; 34].

As evidenced by numerous publications [35–38], the practice of modifying WC–Co hard alloys with Al₂O₃ or ZrO₂ nanoparticles to improve their physical and mechanical characteristics and performance has been in place for a long time. However, to form these particles during sintering, oxide nanoparticles, rather than pure metals, are added to WC-based nanocrystalline powder mixtures, as a rule. There are studies on the effect of Al additives in WC–Co powder mixtures, but they are usually microcrystalline powders with a low content of impurity oxygen; therefore, no Al₂O₃ is formed after sintering and only the presence of intermetallic Al–Co phases is detected [39].

The aim of this study is to find out whether it is possible to prevent strong decarburization of WC in a compacted WC–Co nanocrystalline powder mixture with the help of Al, ZrC, and carbon additives during conventional vacuum sintering and how these additives affect the microstructure and microhardness of the hard alloy.

Materials and Methods

To compensate for the loss of carbon and prevent strong decarburization of WC during vacuum sintering of a hard alloy, the results of using three additives were compared: carbon – to compensate for losses due to decarburization; aluminum – for binding impurity oxygen into solid and refractory oxide Al₂O₃ before its interaction with the carbon of WC; ZrC – to com-

compensate for the loss of carbon and binding of impurity oxygen into refractory oxide ZrO_2 .

The selected additives were introduced into the powder mixture in different amounts, due to the sequence of the experiments and the results obtained. The addition of Al was calculated based on the loss of carbon, which was determined from the change in the phase composition during the sintering of the WC nanopowder (without Co). The sample sintered from the WC nanopowder contained, along with WC, about 7.5 wt. %¹ W_2C , which corresponds to ~0.2 % carbon deficiency (loss) for the formation of single-phase WC. Assuming that the loss of carbon occurred only as a result of interaction with adsorbed oxygen with the formation of CO, at least 0.3 % of oxygen would be required to remove 0.2 % of carbon. To bind 0.3 % oxygen into Al_2O_3 oxide, a minimum of 0.4 % Al is required, taking into account that there is always an oxide film on the surface of Al particles the thickness of which in nanopowders obtained by milling is ~5 nm [40].

The carbon addition was calculated in a similar way, but by the change in the phase composition of the hard alloy made from the WC–6%Co nanocrystalline powder mixture. According to the phase composition of the sintered hard alloy (wt. %: 83.7 WC, 8.2 $\text{Co}_3\text{W}_3\text{C}$, 4.7 $\text{Co}_6\text{W}_6\text{C}$, 3.4 Co_3W), its carbon content does not exceed 5.3 %, while it should be at least 5.8 %. Thus, the addition of carbon to the WC–6%Co powder mixture to compensate for its loss was 0.5 %.

Likewise, the addition of ZrC was also calculated from the change in the phase composition of the hard alloy, but in this case, the possible presence of oxygen on the surface of ZrC nanoparticles after milling was taken into account. Therefore, the case of a sufficient amount of oxygen on the surface of carbide particles to be removed after interaction with the carbide carbon mainly in the form of CO_2 was considered, rather than in the form of CO, as was considered in the case with Al. A minimum of 1.3 % oxygen is required to bind 0.5 % carbon in CO_2 . But to avoid the loss of carbon and completely bind this oxygen in ZrO_2 , at least 4.2 % ZrC is required. Assuming that the interaction of impurity oxygen with carbide carbon can form not only CO_2 , but also CO, 4.0 % of ZrC carbide was added to the WC–6%Co powder mixture before milling.

Nanocrystalline powder mixtures of WC–6%Co with and without additives were prepared using high-energy milling of microcrystalline WC powders ($D_{\text{av}} \approx 6 \mu\text{m}$, $C_{\text{tot}} = 6.15 \%$, $C_{\text{free}} = 0.07 \%$, $O_{\text{tot}} = 0.09 \%$, Kirovgrad hard alloys plant (KZTS), JSC, Kirovgrad), Co ($D_{\text{av}} \approx 3 \mu\text{m}$, KZTS, JSC), Al ($D_{\text{av}} \approx 25 \mu\text{m}$, RUSAL, Krasnoyarsk), ZrC ($D_{\text{av}} \approx 4 \mu\text{m}$, $C_{\text{tot}} = 10.26 \%$, $C_{\text{free}} = 1.72 \%$, $O_{\text{tot}} = 1.40 \%$, Donetsk Plant of Chemical

Reagents, JSC (DZKhR), Donetsk) and carbon black (soot) grade T-900 ($D_{\text{av}} \approx 0.4 \mu\text{m}$, Russia).

Milling of microcrystalline powders taken in a given ratio was carried out using a “Pulverisette 7” planetary ball mill (Fritsch, Germany) using grinding balls and grinding jar lining made of WC–6%Co hard alloy. The same grinding mode was used to prepare all powder mixtures: the rotation speed of the grinding jar support disk was 600 rpm; the weight of the powder taken for grinding was 10 g; the weight of the grinding balls with a diameter of 3 mm ~100 g; grinding jar volume – 45 mL; the volume of isopropyl alcohol $\text{C}_3\text{H}_8\text{O}$ (high purity, 99.9 %, Component-Reaktiv, Ltd, Moscow) added during milling was 10 mL. After milling, the powder mixtures were dried in the vacuum drying cabinet VDL 23 (Binder, Germany) at a pressure of $\sim 10^3 \text{ Pa}$ and a temperature of 85 °C.

The compaction of powder mixtures was carried out at room temperature in a steel cylindrical mold with a punch diameter of 7.45 mm using uniaxial pressing at a pressure of ~460 MPa. Sintering of compact samples placed in graphite crucibles was carried out in a high-temperature vacuum furnace LF-22-2000 (Centorr/Vacuum Industries, USA) for 15 min at $t = 1380 \text{ °C}$ in a vacuum of $\sim 10^{-2} \text{ Pa}$. The heating rate to the temperature of sintering was 10 °C/min.

After sintering, the samples were cut in half along the cross section, the surface of which was then ground and polished on a “Buehler” machine (Germany) using grinding discs and diamond suspensions with a dispersion of 30 to 1 μm .

The crystal structure, phase composition, and lattice parameters of the powders were studied using X-ray diffraction on an XRD-7000 diffractometer (Shimadzu, Japan) with a Bragg–Brentano flat sample arrangement in the angle range 2θ from 10 to 140° with stepwise scanning $\Delta(2\theta) = 0.03^\circ$ and an exposure time of 2 s at a point and $\text{CuK}_{\alpha_{1,2}}$ radiation. The X-ray phase analysis (XPA) of hard alloys was carried out on a STADI-P diffractometer (Stoe, Germany) with a Bragg–Brentano flat sample arrangement in the angle range 2θ from 5 to 120° with stepwise scanning $\Delta(2\theta) = 0.03^\circ$ and $\text{CuK}_{\alpha_{1,2}}$ radiation. The X-ray patterns were analyzed by the Rietveld method using the X'Pert HighScore Plus Version 2.2e software package and the X-ray diffraction data library built into it. The broadening of diffraction reflections of WC was used to determine the average size of coherent scattering regions (DCSR) of X-rays and the magnitude of microstrains (ε).

Chemical analysis of powders for the content of total (C_{tot}) and free (C_{free}) carbon was carried out using a “Metavak CS-30” analyzer (NPO Eksan, Izhevsk). The total oxygen content (O_{tot}) in these powders was determined by reductive melting in a carrier gas flow on an EMGA-620W/C gas analyzer (Horiba, Japan).

¹ Here and elsewhere - wt. %, unless otherwise stated.

The morphology and particle size of powders, as well as the microstructure of hard alloys, were studied using a JSM 6390 LA scanning electron microscope (SEM) (Jeol, Japan) equipped with a JED 2300 analyzer (Jeol, Japan) for Energy Dispersive X-ray (EDX) analysis of the studied area.

The specific surface area (S_{sp}) of the powders was measured by the Brunauer–Emmett–Teller (BET) adsorption method using a “Gemini VII” surface area and porosity analyzer (Micromeritics, USA) after degassing the powders in a vacuum of ~10 Pa at a temperature of 350 °C for 1 h. Assuming the approximation of the same size and spherical shape of particles, the average particle size $D_{BET} = \frac{6}{\rho_{calc} S_{sp}}$, was determined from the measured value S_{sp} , where ρ_{calc} is the density calculated by the mixture rule according to the X-ray phase composition.

The density of hard alloys (ρ_{meas}) was determined using an “AccuPyc II 1340” helium pycno-

meter (Micromeritics, USA) and a measuring chamber with a volume of 1 cm³. The porosity of hard alloys was calculated according to the formula:

$$p = \frac{\rho_{calc} - \rho_{meas}}{\rho_{calc}} \cdot 100 \%$$

The microhardness of hard alloys was measured according to the Vickers method on a MICROMET-1 microhardness tester (Buehler, Germany) with an automatic indentation of a diamond pyramid at a load of 200 g and a the duaration of loading of 10 s. At least 10 measurements (diamond pyramid indentations) were carried out on each sample, after which both diagonals were measured on each indentation, and the average microhardness value and the measurement error were determined from the data obtained.

Results and discussion

The X-ray diffraction patterns of all the initial powders (Fig. 1) used in this work for the preparation of

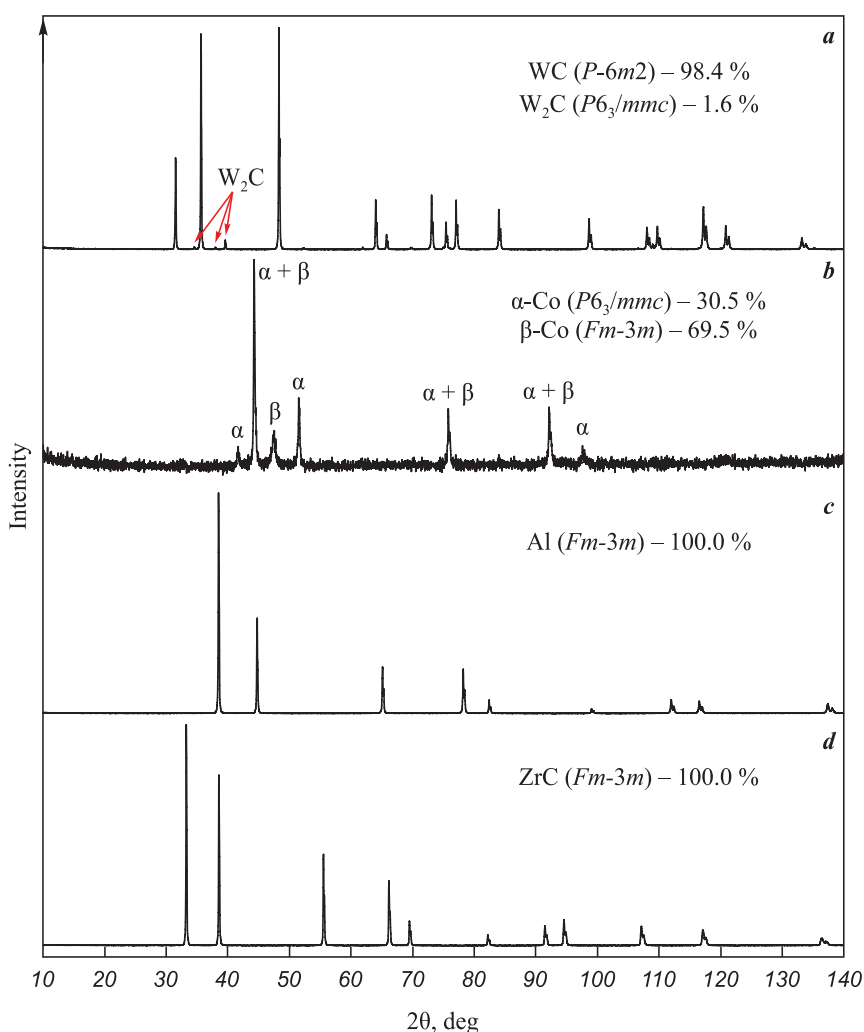


Fig. 1. X-ray diffraction patterns of the initial WC (a), Co (b), Al (c) and ZrC (d) powders

Рис. 1. Рентгенограммы исходных порошков WC (a), Co (b), Al (c) и ZrC (d)

nanocrystalline powder mixtures show rather narrow diffraction reflections, which confirms their coarseness. The WC powder is two-phase (Fig. 1, *a*) and, along with the main phase of hexagonal WC (sp. gr. $P\bar{6}m2$), contains a small amount of lower tungsten carbide W_2C with a hexagonal structure (sp. gr. $P6_3/mmc$), which indicates insufficient content of bound carbon in the W–C system. According to chemical analysis, the content of bound carbon (6.08 %) in WC powder is, indeed, lower than the stoichiometric value (6.13 %), however, there is present free carbon (0.07 %), therefore, the total carbon content in the powder (6.15 %) is sufficient to achieve single-phase WC during sintering. Cobalt Co powder (Fig. 1, *b*) is also two-phase and contains both crystalline modifications: low-temperature (up to 427 °C) α -Co with a hexagonal structure (sp. gr. $P6_3/mmc$) and high-temperature (from 427 to 1495 °C) β -Co with a cubic structure (sp. gr. $Fm\bar{3}m$). Al (Fig. 1, *c*) and ZrC (Fig. 1, *d*) powders are single-

phase and contain only cubic phases (sp. gr. $Fm\bar{3}m$) of Al and ZrC, respectively.

According to SEM images (Fig. 2), the Al powder (Fig. 2, *c*) contains the largest particles (up to 30–40 μm), which are several times larger than the particles of other powders. Co and ZrC powders, on the contrary, appear to be the most dispersed, showing very small rounded particles <1 μm in size, however, most of them are tightly bound together and form large agglomerates with a highly developed surface, ranging in size from hundreds of nanometers to several micrometers (Fig. 2, *b*, *d*). The WC powder (Fig. 2, *a*) is similar in particle morphology to Al powder (Fig. 2, *c*), but is closer to Co and ZrC powders in particle size and their agglomerates (Fig. 2, *b*, *d*).

Table 1 shows the average, maximum, and minimum particle sizes of the initial powders, determined from their SEM images, as well as their specific surface and the average particle size calculated from it.

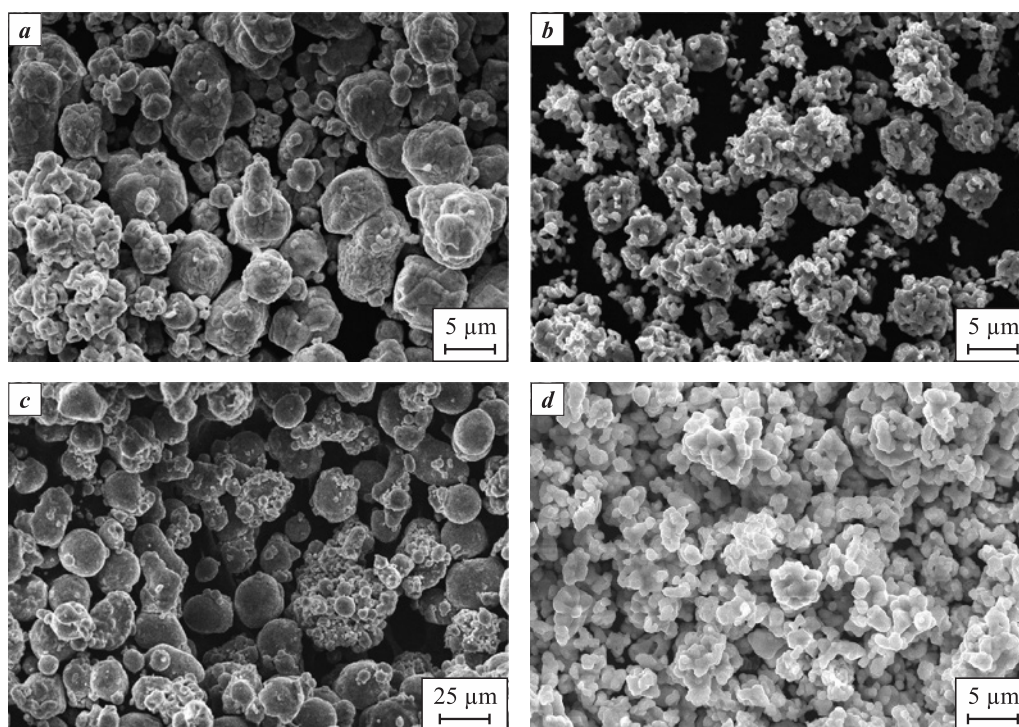


Fig. 2. SEM images of the initial WC (*a*), Co (*b*), Al (*c*) and ZrC (*d*) powders

Рис. 2. СЭМ-изображения исходных порошков WC (*a*), Co (*b*), Al (*c*) и ZrC (*d*)

Table 1. Characteristics of initial powders

Таблица 1. Характеристики исходных порошков

Powder	D_{av} , μm	D_{min} , μm	D_{max} , μm	S_{sp} , m^2/g	ρ_{calc} , g/cm^3	D_{BET} , μm
WC	3.03	0.52	12.08	0.19 ± 0.01	15.70	1.97
Co	1.37	0.30	4.48	0.98 ± 0.01	8.80	0.69
Al	7.91	0.70	36.36	0.37 ± 0.02	2.70	6.02
ZrC	1.83	0.39	5.98	0.68 ± 0.01	6.63	1.32

After preparation, all powder mixtures, according to X-ray diffraction (Fig. 3) and SEM (Fig. 4), look the same. The X-ray diffraction patterns of the mixtures (Fig. 3) show the same reflections as for the initial WC powder (see Fig. 1, *a*), which belong to the WC and W_2C phases. However, due to the small size of the CSR and the presence of microdeformations, the diffraction reflections in the X-ray diffraction patterns of powder mixtures are noticeably broadened, due to

which weak reflections of Co and Al or ZrC, are not visible. A quantitative analysis of the broadening of WC reflections showed that the average CSR sizes and microstrains for WC particles in all powder mixtures have close values (Table 2). The same is observed on the SEM images (Fig. 4), where powder mixtures have very little differences both in terms of particle size and morphology, although the initial powders were considerably different, especially Al powder (see Fig. 2).

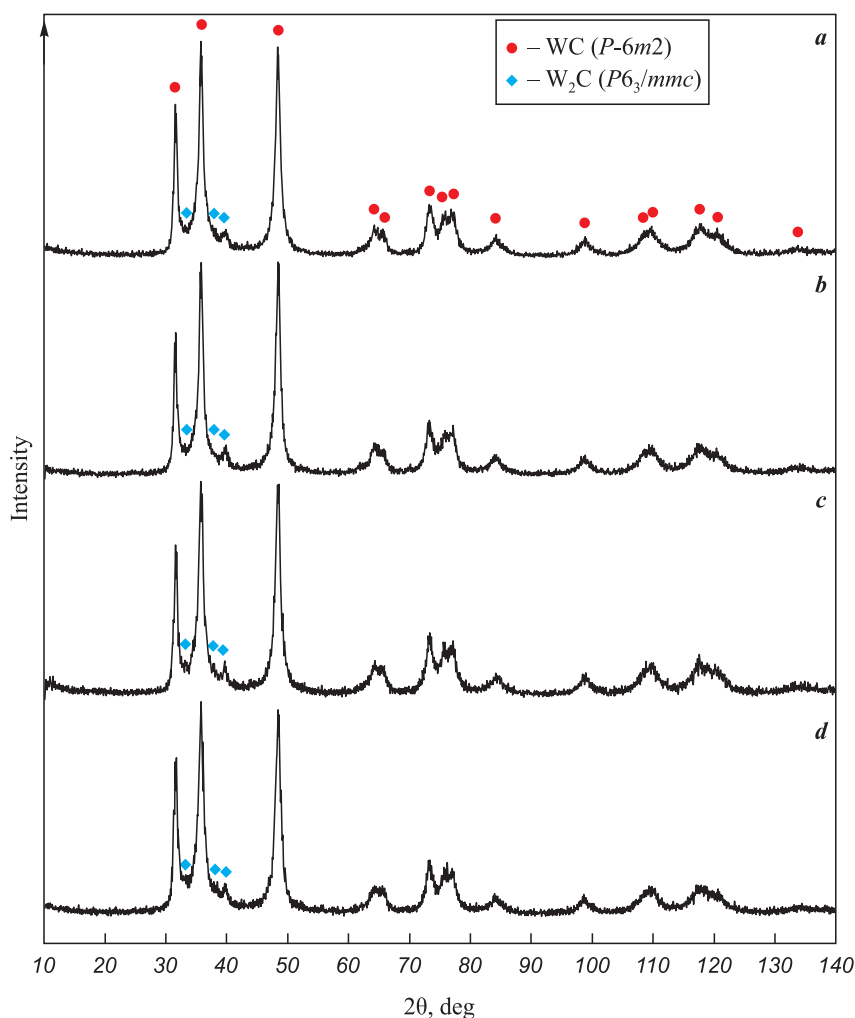


Fig. 3. X-ray diffraction patterns of nanocrystalline powder mixtures WC-6Co (*a*), WC-6Co-0.5C (*b*), WC-6Co-0.4Al (*c*) and WC-6Co-4ZrC (*d*)

Рис. 3. Рентгенограммы нанокристаллических порошковых смесей WC-6Co (*a*), WC-6Co-0,5C (*b*), WC-6Co-0,4Al (*c*) и WC-6Co-4ZrC (*d*)

Table 2. Characteristics of nanocrystalline powder mixtures

Таблица 2. Характеристики нанокристаллических порошковых смесей

Powder	O _{tot} , wt. %	S _{sp} , m ² /g	ρ _{calc} , g/cm ³	D _{BET} , nm	D _{CSR} , nm	ε, %
WC-6Co	3.3 ± 0.1	5.81 ± 0.05	14.99	69	47	0.81
WC-6Co-0.5C	3.4 ± 0.1	5.03 ± 0.04	14.49	82	34	0.70
WC-6Co-0.4Al	4.2 ± 0.1	8.12 ± 0.06	14.74	50	33	0.75
WC-6Co-4ZrC	4.3 ± 0.1	9.64 ± 0.06	14.25	44	39	0.88

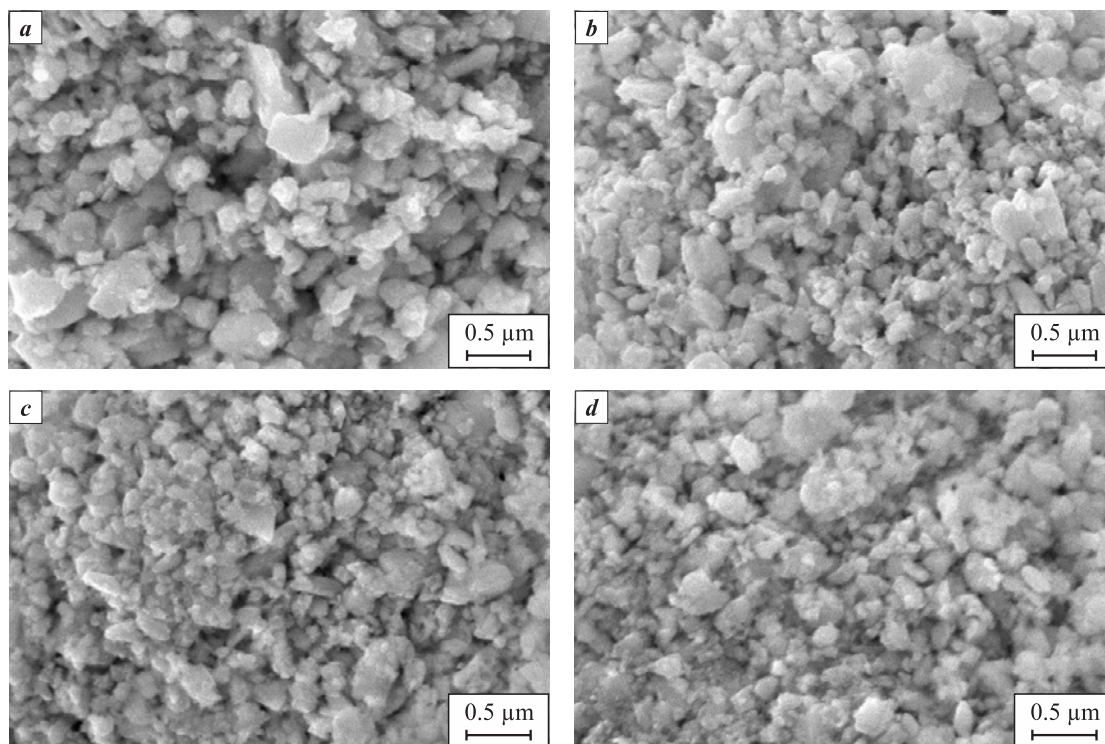


Fig. 4. SEM images of powder mixtures

WC-6Co (a), WC-6Co-0.5C (b), WC-6Co-0.4Al (c) and WC-6Co-4ZrC (d)

Рис. 4. СЭМ-изображения порошковых смесей

WC-6Co (a), WC-6Co-0,5C (b), WC-6Co-0,4Al (c) и WC-6Co-4ZrC (d)

Thus, all the additives used in this work not only did not affect the grinding of WC, but themselves turned out to be grinded and subjected to grinding and uniform distribution throughout the volume of the powder mixture, including Al. This is also confirmed by the values of the specific surface area of powder mixtures (Table 2), which are an order of magnitude higher than the values for the initial powders (Table 1), whereas the average particle sizes in the mixtures calculated from the specific surface turned out to be close in magnitude to the average CSR sizes and do not exceed 100 nm (Table 2). It should be noted, however, that the additives introduced into the powder mixture, as expected, also introduced additional oxygen; its measured total content in nanocrystalline powder mixtures significantly exceeds the amount estimated based on the change in the phase composition (Table 2).

Despite the similarity of the obtained powder mixtures, hard alloys sintered from them significantly differ from each other both in phase composition (Fig. 5) and in microstructure (Fig. 6). On the X-ray diffraction pattern of the WC-6Co hard alloy (Fig. 5, a), which was sintered from the WC-6%Co powder mixture without any additives, diffraction reflections of three other phases are clearly visible in addition to the main phase WC, which indicate a carbon deficiency and are extremely undesirable in a hard alloy [41].

The addition of carbon to the powder mixture almost completely made up for its deficiency in the sintered hard alloy, its X-ray diffraction pattern of the main WC and Co phases are observed, however, weak lines of the $\text{Co}_3\text{W}_3\text{C}$ η -phase are still present (Fig. 5, b). The addition of aluminum, on the contrary, only exacerbated the consequences of carbide decarburization, as a result of which the qualitative phase composition of the alloy became similar to the composition of the hard alloy from a powder mixture without additives (Fig. 5, a), while the content of undesirable phases increased (Fig. 5, c). Probably, during the preparation of the WC-6Co-0.4Al powder mixture, all the aluminium introduced was completely oxidized to Al_2O_3 during intensive grinding, and while sintering, instead of binding the oxygen adsorbed on the carbide particles, it, on the contrary, brought additional oxygen to its surface, resulting in an even greater loss of carbon. The addition of ZrC to the powder mixture allowed to preserve fully the WC and Co phases in the hard alloy sintered from the mixture, binding most of the adsorbed oxygen into the monoclinic ZrO_2 oxide, as evidenced by the X-ray phase composition of the sintered alloy (Fig. 5, d).

According to the XRD results of hard alloys, the assessment of carbon loss ($\sim 0.5\%$) and the amount of oxygen involved ($\sim 1.3\%$) based on the change in

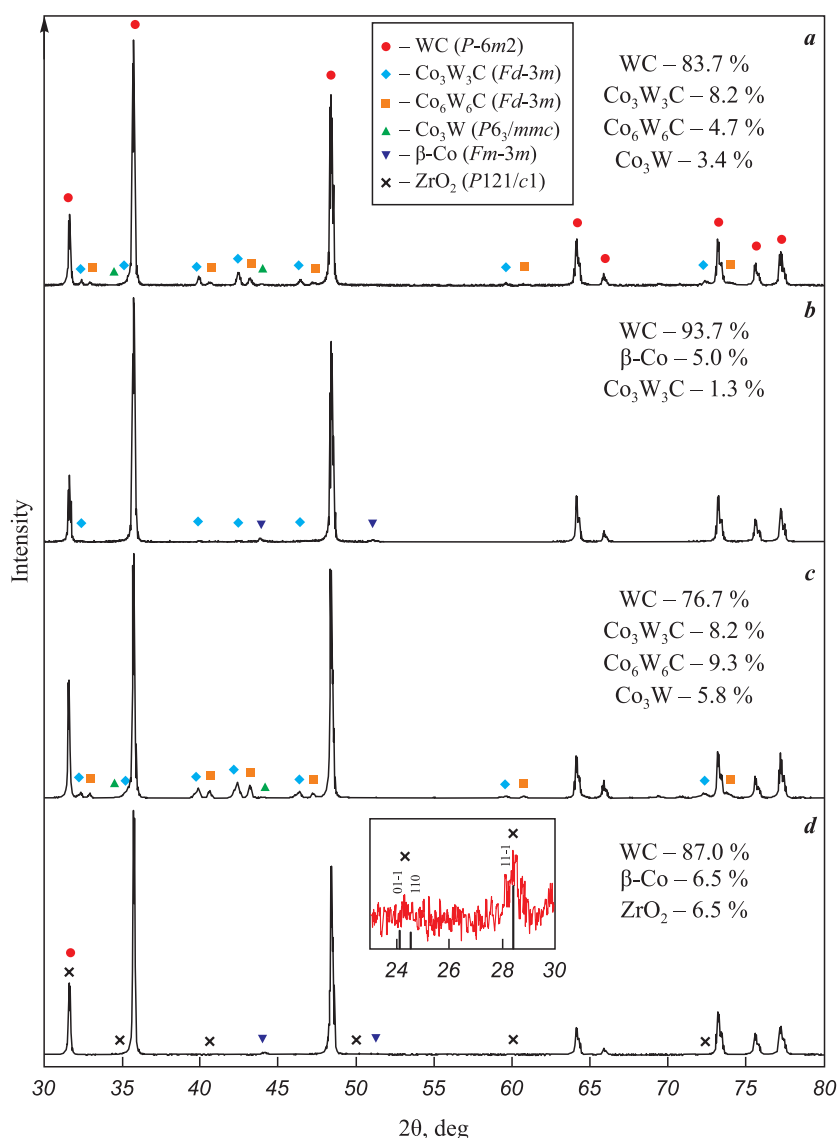


Fig. 5. X-ray diffraction patterns of hard alloys

WC-6Co (a), WC-6Co-0.5C (b), WC-6Co-0.4Al (c), and WC-6Co-4ZrC (d)

The inset shows an enlarged fragment of the X-ray diffraction pattern with the most intense (11-1) line of the ZrO₂ phase

Рис. 5. Рентгенограммы твердых сплавов

WC-6Co (a), WC-6Co-0,5C (b), WC-6Co-0,4Al (c) и WC-6Co-4ZrC (d)

На вставке – увеличенный фрагмент рентгенограммы с наиболее интенсивной линией (11-1) фазы ZrO₂

the phase composition allowed for fairly accurate calculation of the amount of carbon and ZrC additives required to prevent WC decarburization. However, the measured total oxygen content in nanocrystalline powder mixtures (see Table 2) turned out to be several-fold higher than the estimated one. This means that only a part of the oxygen contained in the powder mixture is in the chemisorbed state, while the rest is present in other forms, including in the form of physically adsorbed water, which is removed upon heating without taking part in the decarburization of WC.

The microstructure of the WC-6Co alloy sintered from a powder mixture without additives (Fig. 6, a) looks rather dense and includes WC grains (light-

colored), the space between which is filled with cobalt-containing phases (dark-colored) detected by X-ray diffraction (Fig. 5, a), and a few pores (black) no larger than 1 μm in size. Only WC grains and their intergrowths separated by a cobalt binder are observed in the microstructure of the WC-6Co-0.5C hard alloy sintered from a powder mixture with the addition of carbon (Fig. 6, b). As can be seen from XRD-analysis, the addition of Al to the powder mixture filled the microstructure of the hard alloy sintered from it (Fig. 6, c) with a large number of rounded inclusions (black-colored), resembling pores, among the grains of WC (light-colored) and cobalt-containing phases (dark-colored), (Fig. 5, c). The EDX analysis

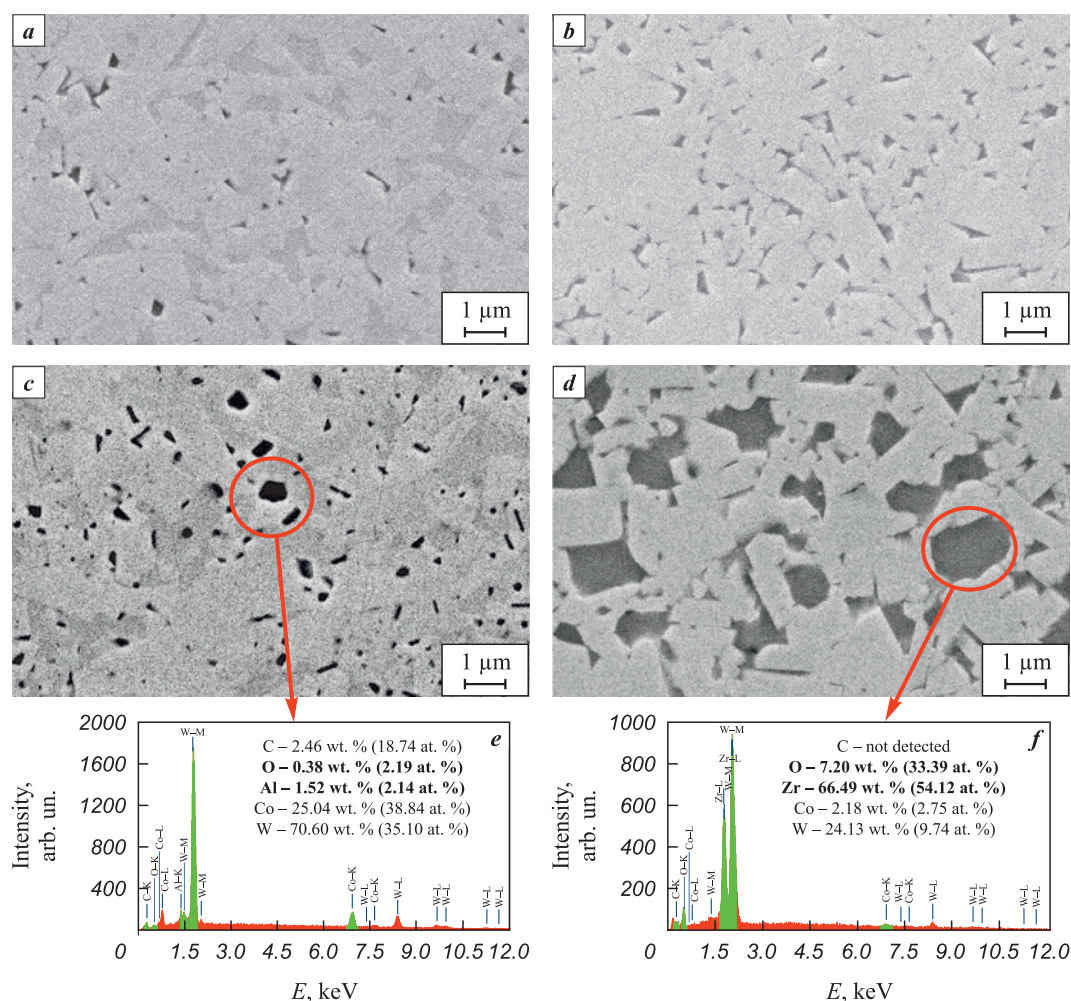


Fig. 6. SEM images of hard alloys
WC-6Co (a), WC-6Co-0.5C (b), WC-6Co-0.4Al (c) and WC-6Co-4ZrC (d)
and the results of EDX analysis of the selected areas (e, f)

Рис. 6. СЭМ-изображения твердых сплавов
WC-6Co (a), WC-6Co-0,5C (b), WC-6Co-0,4Al (c) и WC-6Co-4ZrC (d)
и результаты EDX-анализа выделенных областей (e, f)

Table 3. Characteristics of sintered hard alloys

Таблица 3. Характеристики спеченных твердых сплавов

Sample	D_{av} , μm	D_{min} , μm	D_{max} , μm	HV , GPa	ρ_{meas} , g/cm ³	ρ_{calc} , g/cm ³	p , %
WC-6Co	0.80	0.14	2.57	19.3 ± 0.8	15.14 ± 0.01	15.41	1.8
WC-6Co-0.5C	0.84	0.21	3.23	18.4 ± 0.5	15.03 ± 0.01	15.07	0.3
WC-6Co-0.4Al	0.78	0.25	1.63	18.0 ± 1.0	14.76 ± 0.01	14.99*	1.5
WC-6Co-4ZrC	1.08	0.28	4.43	17.2 ± 0.9	13.79 ± 0.01	13.86*	0.5

* Taking into account that Al and ZrC transformed completely into Al₂O₃ and ZrO₂.

showed that the rounded dark areas observed in the microstructure of the WC-6Co-0.4Al hard alloy contain aluminum and oxygen (Fig. 6, c, e) and are Al₂O₃ particles and not pores. The authors of [36] reported similar inclusions in the WC-3Co-3Al₂O₃ alloy, detected using field emission scanning microscopy (FESEM) and EDX mapping (MAP), which showed

that these are Al₂O₃. The microstructure of the hard alloy (Fig. 6, d) made from a powder mixture with the addition of ZrC is a dense composition of carbide WC (light-colored) and oxide ZrO₂ (dark-colored) grains surrounded by a cobalt layer, as confirmed by the EDX (Fig. 6, f) and XFA (Fig. 5, d) analysis. Though in the WC-6Co-4ZrC powder mixture WC and ZrC

nanoparticles are distributed uniformly over the entire volume, as it can be seen from the SEM images (Fig. 4, *d*), individual microcrystalline ZrO_2 and WC grains formed in the microstructure of the hard alloy sintered from the powder, i.e. the growth of grains of various phases was not limited, as expected, on the contrary, it was supported.

Table 3 shows the average, minimum, and maximum WC grain sizes determined from several SEM images for each hard alloy. According to these data, the carbon deficiency in the alloy inhibits the growth of WC grains, especially in the presence of Al_2O_3 particles, while the addition of carbon or ZrC, quite the contrary, promotes the growth of carbide grains, as confirmed by the average and maximum grain sizes in the hard alloy (Table 3). It is known that the presence of free carbon promotes the growth of WC grains during sintering, especially in the case of liquid-phase sintering [42]. According to [43; 44], during the oxidation of ZrC, there is a dissolution of oxygen in the carbide lattice; it is first accompanied by the formation of oxycarbide with the release of free carbon and zirconium from the carbide lattice; as oxygen further dissolves, the oxycarbide transforms into the cubic ZrO_2 phase containing a certain amount of carbon, and then upon complete oxidation, it transforms into the ZrO_2 monoclinic phase, which is seen in the *X*-ray diffraction pattern of the hard alloy (Fig. 5, *d*). Unlike ZrC, during the oxidation of WC, carbon leaves the carbide lattice in the form of CO/CO_2 , leading to its decarburization [43; 45]. Thus, heating of the WC–6Co–4ZrC powder mixture, ZrC carbide not only binds the adsorbed oxygen into ZrO_2 oxide, but also compensates for the loss of carbon in WC, as is the case with the addition of carbon in the WC–6Co–0.5C mixture.

The additives used not only affected the microstructure of the hard alloy, but also led to a decrease in its density and microhardness (Table 3). The calculated density of the hard alloy with the WC–6Co phase composition is 14.97 g/cm^3 . However, due to the loss of carbon during sintering and the resulting formation of undesirable phases (Fig. 5, *a*), the density of the WC–6Co hard alloy (both calculated and measured) exceeded the expected one. The hard alloy WC–6Co–0.5C turned out to be closest to the WC–6Co hard alloy both in terms of phase composition and density. As *X*-ray diffraction patterns of hard alloys produced from powder mixtures WC–6Co–0.4Al and WC–6Co–4ZrC did not show reflections of the initial phases (Al or ZrC), while inclusions close in composition to Al_2O_3 and ZrO_2 were found in the microstructure, the density of the samples ρ_{calc} was calculated from the *X*-ray phase composition, taking into account the amount of oxide, into which the entire additive could turn. Calculations and measured density values

of hard alloys showed that additions of carbon and ZrC, making up for the loss of carbon during sintering, contribute to the formation of a microstructure with the lowest porosity compared to carbon-deficient hard alloys (Table 3).

Besides, the deviation of the phase composition of the hard alloy from the perfect WC–6Co is accompanied by an increase in the inhomogeneity (scatter of values) of its microhardness, as confirmed by the measured value's error (Table 3). Overall, the measurements have shown that carbon deficiency leads to an increase in microhardness, while the presence of Al_2O_3 and ZrO_2 oxide inclusions in the hard alloy microstructure, on the contrary, reduces it.

Conclusion

Homogeneous nanocrystalline powder mixtures with the average particle size not exceeding 100 nm based on WC–6Co with and without additives of C, Al, ZrC were prepared by high-energy milling from crystalline powders differing in their composition, properties, quantity, and average particle size. In the obtained mixtures, a high oxygen content was found; the amount of oxygen increases with the introduction of additives, especially Al. Though the original aluminum powder contained very large particles, it was completely oxidized during milling and turned into nanocrystalline oxide Al_2O_3 ; this fact only increased the loss of carbon during sintering and led to the formation of a multiphase and relatively porous microstructure of the hard alloy.

It was shown that only a part of oxygen contained in the powder mixtures is in the chemisorbed state and takes part in the decarburization of WC during vacuum sintering. The use of carbon and ZrC additives allowed to prevent the decarburization of WC during sintering of the hard alloy and to form a less porous microstructure in it. However, even the presence of ZrO_2 inclusions could not impede the intensive growth of WC grains during sintering, on the contrary, it rather promoted it. Besides, the microhardness measurements have shown that carbon deficiency leads to an increase in microhardness, while the presence of Al_2O_3 and ZrO_2 oxide inclusions in the hard alloy microstructure, on the contrary, reduces it.

References / Список литературы

1. Samoilov V.S., Eikhmans E.F., Fal'kovskii V.A., Loktev A.D., Shkurin Yu.P. Metalworking carbide tools: Handbook. Moscow: Mashinostroyeniye, 1988. 368 p. (In Russ.).
Самойлов В.С., Эйхманс Э.Ф., Фальковский В.А., Локтев А.Д., Шкурин Ю.П. Металлообрабатывающий



- твердосплавный инструмент: Справочник. М.: Машиностроение, 1988. 368 с.
2. Falkovskii V.A., Klyachko L.I. Hard alloys. Moscow: Publ. Ruda i metally, 2005, 413 p. (In Russ.).
Фальковский В.А., Клячко Л.И. Твердые сплавы. М.: Изд. дом «Руда и металлы», 2005. 413 с.
3. Panov V.S., Chuvilin A.M. Technology and properties of sintered hard alloys and products from them. Moscow: MISIS, 2001, 432 p. (In Russ.).
Панов В.С., Чувилин А.М. Технология и свойства спеченных твердых сплавов и изделий из них. Учеб. пос. для вузов. М.: МИСИС, 2001. 432 с.
4. Lassner E., Schubert W.D. Tungsten compounds and their application. In: *Tungsten: Properties, chemistry, technology of the element, alloys, and chemical compounds*. Boston: Springer, MA, 1999. P. 133–177.
https://doi.org/10.1007/978-1-4615-4907-9_4
5. Sarin V.K. Comprehensive hard materials. Oxford: Elsevier, 2014. 1806 p.
6. Gusev A.I., Kurlov A.S. Mechanical milling process modeling and making WC nanocrystalline powder. *Inorganic Materials*. 2009;45:35–42.
<https://doi.org/10.1134/S0020168509010063>
Гусев А.И., Курлов А.С. Моделирование процесса механического размолла и получение нанокристаллического порошка WC. *Неорганические материалы*. 2009;45(1):38–45.
7. El-Eskandarany M.S., Mahday A.A., Ahmed H.A., Amer A.H. Synthesis and characterizations of ball-milled nanocrystalline WC and nanocomposite WC–Co powders and subsequent consolidations. *Journal of Alloys and Compounds*. 2000;312(1–2):315–325.
[https://doi.org/10.1016/S0925-8388\(00\)01155-5](https://doi.org/10.1016/S0925-8388(00)01155-5)
8. Isaeva N.V., Blagoveshchenskii Yu.V., Blagoveshchenskaya N.V., Mel'nik Yu.I., Samokhin A.V., Alekseev N.V., Astashov A.G. Preparation of nanopowders of carbides and hard-alloy mixtures applying low-temperature plasma. *Russian Journal of Non-Ferrous Metals*. 2014;55(6):585–591.
<https://doi.org/10.3103/S1067821214060108>
Исаева Н.В., Благовещенский Ю.В., Благовещенская Н.В., Мельник Ю.И., Самохин А.В., Алексеев Н.В., Асташов А.Г. Получение нанопорошков карбидов и твердосплавных смесей с применением низкотемпературной плазмы. *Известия вузов. Порошковая металлургия и функциональные покрытия*. 2013;(3):7–14.
<https://doi.org/10.17073/1997-308X-2013-3-7-14>
9. McChandlish L.E., Seegoraul P. Development and applications of nanostructured tungsten carbide/cobalt powders. In: *Proceedings of the European Conference on Advances in Hard Materials*, Stockholm, 1996. P. 93–100.
10. Gao L., Kear B.H. Low temperature carburization of high surface area tungsten powders. *Nanostructured Materials*. 1995;5(5):555–569.
[https://doi.org/10.1016/0965-9773\(95\)00265-G](https://doi.org/10.1016/0965-9773(95)00265-G)
11. Fabijanić T.A., Alar Z., Čorić D. Influence of consolidation process and sintering temperature on microstructure and mechanical properties of near nano- and nano-structured WC–Co cemented carbides. *International Journal of Refractory Metals and Hard Materials*. 2016;54:82–89.
<https://doi.org/10.1016/j.jrmhm.2015.07.017>
12. Breval E., Cheng J.P., Agrawal D.K., Gigl P., Dennis M., Roy R., Papworth A.J. Comparison between microwave and conventional sintering of WC/Co composites. *Materials Science and Engineering: A*. 2005;391(1–2): 285–295.
<https://doi.org/10.1016/j.msea.2004.08.085>
13. Chuvil'deev V.N., Moskvicheva A.V., Boldin M.S., Sakharov N.V., Blagoveshchenskii Yu.V., Isaeva N.V., Mel'nik Yu.I., Shotin S.V., Nokhrin A.V. Spark plasma sintering of nanostructured tungsten carbide and carbide alloys. *Vestnik of Lobachevsky University of Nizhni Novgorod*. 2013;2(2):115–119. (In Russ.).
Чувильдеев В.Н., Москвичева А.В., Болдин М.С., Сахаров Н.В., Благовещенский Ю.В., Исаева Н.В., Мельник Ю.И., Шотин С.В., Нохрин А.В. Электроимпульсное плазменное спекание наноструктурированного карбида вольфрама и твердых сплавов на его основе. *Вестник Нижегородского университета им. Н.И. Лобачевского*. 2013;2(2):115–119.
14. Kim H.C., Shon I.J., Jeong I.K., Ko I.Y., Yoon J.K., Doh J.M. Rapid sintering of ultra fine WC and WC–Co hard materials by high-frequency induction heated sintering and their mechanical properties. *Metals and Materials International*. 2007;13(1):39–45.
<https://doi.org/10.1007/BF03027821>
15. Kelto C.A., Timm E.E., Pyzik A.J. Rapid omnidirectional compaction (ROC) of powder. *Annual Review of Materials Science*. 1989;19:527–550.
<https://doi.org/10.1146/annurev.ms.19.080189.002523>
16. Raihanuzzaman R.M., Rosinski M., Xie Z., Ghomashchi R. Microstructure and mechanical properties and of pulse plasma compacted WC–Co. *International Journal of Refractory Metals and Hard Materials*. 2016;60:58–67.
<https://doi.org/10.1016/j.jrmhm.2016.07.002>
17. Wang X., Fang Z., Sohn H.Y. Nanocrystalline cemented tungsten carbide sintered by an ultra-high-pressure rapid hot consolidation process. In: *Proceedings of the 2007 International Conference on Powder Metallurgy & Particulate Materials*. Ed. J. Engquist. Denver, US, 2007;2:08–01.
18. Krokhaliev A.V., Kharlamov V.O., Tupitsin M.A., Kuzmin S.V., Lysak V.I. Revisiting the possibility of formation of hard alloys from powder mixtures of carbides with metals by explosive compacting without sintering. *Russian Journal of Non-Ferrous Metals*. 2018;59(5):550–556.
<https://doi.org/10.3103/S1067821218050073>
Крохалев А.В., Харламов В.О., Тупицин М.А., Кузьмин С.В., Лысак В.И. О возможности получения твердых сплавов из смесей порошков карбидов с металлами взрывным прессованием без спекания. *Известия вузов. Порошковая металлургия и функциональные покрытия*. 2017;(2):22–30.
<https://doi.org/10.17073/1997-308X-2017-2-22-30>
19. Raihanuzzaman R.M., Xie Z., Hong S.J., Ghomashchi R. Powder refinement, consolidation and mechanical properties of cemented carbides: An overview. *Powder Technology*. 2014;261:1–13.
<https://doi.org/10.1016/j.powtec.2014.04.024>
20. Blagoveshchenskiy Y.V., Isayeva N.V., Blagoveshchenskaya N.V., Melnik Yu.I., Chuvildeev V.N., Nokhrin A.V., Sakharov N.V., Boldin M.S., Smirnov Ye.S., Shotin S.V., Levinsky Yu.V., Voldman G.M. Methods of compacting

- nanostructured tungsten-cobalt alloys from nanopowders obtained by plasma chemical synthesis. *Inorganic Materials: Applied Research*. 2015;6(5):415–426.
<https://doi.org/10.1134/S2075113315050032>
- Благовещенский Ю.В., Исаева Н.В., Благовещенская Н.В., Мельник Ю.И., Чуви́льдеев В.Н., Нохрин А.В., Сахаров Н.В., Болдин М.С., Смирнова Е.С., Шотин С.В., Левинский Ю.В., Вольдман Г.М. Методы компактирования наноструктурных вольфрам-кобальтовых сплавов из нанопорошков, полученных методом плазмохимического синтеза. *Перспективные материалы*. 2015;(1):5–21.
21. Norgren S., García J., Blomqvist A., Yin L. Trends in the P/M hard metal industry. *International Journal of Refractory Metals and Hard Materials*. 2015;48:31–45.
<https://doi.org/10.1016/j.ijrmhm.2014.07.007>
 22. García J., Ciprés V.C., Blomqvist A., Kaplan B. Cemented carbide microstructures: A review. *International Journal of Refractory Metals and Hard Materials*. 2019;80:40–68.
<https://doi.org/10.1016/j.ijrmhm.2018.12.004>
 23. Fang Z.Z., Wang X., Ryu T., Hwang K.S., Sohn H.Y. Synthesis, sintering, and mechanical properties of nanocrystalline cemented tungsten carbide: A review. *International Journal of Refractory Metals and Hard Materials*. 2009;27:288–299. <https://doi.org/10.1016/j.ijrmhm.2008.07.011>
 24. Krasovskii P.V., Blagoveshchenskii Y.V., Grigorovich K.V. Determination of oxygen in W–C–Co nanopowders. *Inorganic Materials*. 2008;44(9):954–959.
<https://doi.org/10.1134/S0020168508090100>
- Красовский П.В., Благовещенский Ю.В., Григорович К.В. Определение содержания кислорода в нанопорошках системы W–C–Co. *Неорганические материалы*. 2008;44(9):1074–1079.
25. Kurlov A.S. Effects of vacuum annealing on the particle size and phase composition of nanocrystalline tungsten carbide powders. *Russian Journal of Physical Chemistry A*. 2013;87(4):654–661.
<https://doi.org/10.1134/S0036024413040158>
- Курлов А.С. Влияние вакуумного отжига на размер частиц и фазовый состав нанокристаллических порошков WC. *Журнал физической химии*. 2013;87(4):664–671. <https://doi.org/10.7868/S0044453713040158>
26. Lantsev E.A., Malekhonova N.V., Tsvetkov Yu.V., Blagoveshchensky Yu.V., Chuvildeev V.N., Nokhrin A.V., Boldin M.S., Andreev P.V., Smetanina K.E., Isaeva N.V. Investigation of aspects of high-speed sintering of plasma-chemical nanopowders of tungsten carbide with higher content of oxygen. *Inorganic Materials: Applied Research*. 2021;12(3):650–663.
<https://doi.org/10.1134/S2075113321030242>
- Ланцев Е.А., Малехонова Н.В., Цветков Ю.В., Благовещенский Ю.В., Чуви́льдеев В.Н., Нохрин А.В., Болдин М.С., Андреев П.В., Сметанина К.Е., Исаева Н.В. Исследование особенностей высокоскоростного спекания плазмохимических нанопорошков карбида вольфрама с повышенным содержанием кислорода. *Физика и химия обработки материалов*. 2020;(6):23–39.
<https://doi.org/10.30791/0015-3214-2020-6-23-39>
27. Kurlov A.S., Gusev A.I., Rempel' A.A. Vacuum sintering of WC–8wt.%Co hardmetals from WC powders with different dispersity. *International Journal of Refractory Metals and Hard Materials*. 2011;29(2):221–231.
<https://doi.org/10.1016/j.ijrmhm.2010.10.010>
 28. Kurlov A.S., Rempel' A.A., Blagoveshenskii Y.V., Samokhin A.V., Tsvetkov Yu.V. Hard alloys WC–Co (6 wt %) and WC–Co (10 wt %) based on nanocrystalline powders. *Doklady Chemistry*. 2011;439(1):213–218.
<https://doi.org/10.1134/S0012500811070068>
- Курлов А.С., Ремпель А.А., Благовещенский Ю.В., Самохин А.В., Цветков Ю.В. Твердые сплавы WC–6 мас.%Co и WC–10 мас.%Co на основе нанокристаллических порошков. *Доклады Академии наук*. 2011;439(2):215–220.
29. Lantsev E.A., Malekhonova N.V., Nokhrin A.V., Chuvildeev V.N., Boldin M.S., Andreev P.V., Smetanina K.E., Blagoveshchenskiy Yu.V., Isaeva N.V., Murashov A.A. Spark plasma sintering of fine-grained WC hard alloys with ultra-low cobalt content. *Journal of Alloys and Compounds*. 2021;857:157535.
<https://doi.org/10.1016/j.jallcom.2020.157535>
 30. Kurlov A.S., Yumasheva N.D., Danilov D.A. Concentration of oxygen and forms of it in TaC nanopowders. *Russian Journal of Physical Chemistry A*. 2019;93(3):501–508.
<https://doi.org/10.1134/S0036024419030117>
- Курлов А.С., Юмашева Н.Д., Данилов Д.А. Содержание кислорода и формы его существования в нанопорошках TaC. *Журнал физической химии*. 2019;93(3):405–413.
<https://doi.org/10.1134/S0044453719030117>
31. Kurlov A.S., Yumasheva N.D., Danilov D.A. Vacuum annealing of TaC nanopowders. *Russian Journal of Physical Chemistry A*. 2020;94(7):1447–1455.
<https://doi.org/10.1134/S0036024420070183>
- Курлов А.С., Юмашева Н.Д., Данилов Д.А. Вакуумный отжиг нанопорошков TaC. *Журнал физической химии*. 2020;94(7):1083–1092.
<https://doi.org/10.31857/S0044453720070183>
32. Bokov A., Shelyug A., Kurlov A. Interplay between decarburization, oxide segregation, and densification during sintering of nanocrystalline TaC and NbC. *Journal of the European Ceramic Society*. 2021;41(12):5801–5812.
<https://doi.org/10.1016/j.jeurceramsoc.2021.05.007>
 33. Abyzov A.M. Aluminum oxide and alumina ceramics (Review). Pt. 1. Properties of Al₂O₃ and commercial production of dispersed Al₂O₃. *Refractories and Industrial Ceramics*. 2019;60(1):24–32.
<https://doi.org/10.1007/s11148-019-00304-2>
- Абызов А.М. Оксид алюминия и алюмооксидная керамика (Обзор). Ч. 1. Свойства Al₂O₃ и промышленное производство дисперсного Al₂O₃. *Новые огнеупоры*. 2019;(1):16–23. <https://doi.org/10.17073/1683-4518-2019-1-16-23>
34. Zhigachev A.O., Golovin Yu.I., Umrikhin A.V., Korenkov V.V., Tyurin A.I., Rodaev V.V., Dyachek T.A. Ceramic materials based on zirconium dioxide. Moscow: Tekhnosfera. 2018, 358 p. (In Russ.).
- Жигачев А.О., Головин Ю.И., Умрихин А.В., Коренков В.В., Тюрин А.И., Родаев В.В., Дьячек Т.А. Керамические материалы на основе диоксида циркония. М.: Техносфера, 2018. 358 с.
35. Gordeev Yu.I., Abkaryan A.K., Zeer G.M. Design and investigation of hard metals and ceramics composites

- modified by nanoparticles. *Perspektivnye materialy*. 2012;(5):76–88. (In Russ.).
- Гордеев Ю.И., Абкарян А.К., Зеер Г.М. Конструирование и исследование твердосплавных и керамических композитов, модифицированных наночастицами. *Перспективные материалы*. 2012;(5):76–88.
36. Fazili A., Nikzad L., RahimiPour M.R., Razavi M., Salahi E. Effect of Al_2O_3 ceramic binder on mechanical and microstructure properties of spark plasma sintered WC–Co cermets. *International Journal of Refractory Metals and Hard Materials*. 2017;69:189–195. <https://doi.org/10.1016/j.ijrmhm.2017.08.010>
 37. Mukhopadhyay A., Chakravarty D., Basu B. Spark plasma-sintered WC–ZrO₂–Co nanocomposites with high fracture toughness and strength. *Journal of the American Ceramic Society*. 2010;93(6):1754–1763. <https://doi.org/10.1111/j.1551-2916.2010.03685.x>
 38. Xia X., Li X., Li J., Zheng D. Microstructure and characterization of WC–2.8wt% Al_2O_3 –6.8wt% ZrO₂ composites produced by spark plasma sintering. *Ceramics International*. 2016;42(12):14182–14188. <https://doi.org/10.1016/j.ceramint.2016.06.044>
 39. Arenas F.J., Matos A., Cabezas M., Rauso C.D., Grigorescu C. Densification, mechanical properties and wear behavior of WC–VC–Co–Al hardmetals. *International Journal of Refractory Metals and Hard Materials*. 2001;19(4–6):381–387. [https://doi.org/10.1016/S0263-4368\(01\)00014-2](https://doi.org/10.1016/S0263-4368(01)00014-2)
 40. André B., Coulet M.-V., Esposito P.-H., Rufino B., Denoyel R. High-energy ball milling to enhance the reactivity of aluminum nanopowders. *Materials Letters*. 2013;110:108–110. <https://doi.org/10.1016/j.matlet.2013.07.101>
 41. Kurlov A.S., Gusev A.I. Tungsten carbides: Structure, properties and application in hardmetals. In: *Tungsten carbides*. (Springer series in materials science). Vol. 184. Springer, Cham., 2013. 242 p. <https://doi.org/10.1007/978-3-319-00524-9>
 42. Konyashin I., Hlawatschek S., Ries B., Lachmann F., Dorn F., Sologubenko A., Weirich T. On the mechanism of WC coarsening in WC–Co hardmetals with various carbon contents. *International Journal of Refractory Metals and Hard Materials*. 2009;27(2):234–243. <https://doi.org/10.1016/j.ijrmhm.2008.09.001>
 43. Voitovich R.F. Oxidation of carbides and nitrides. Kiev: Naukova dumka. 1981, 192 p. (In Russ.).
Войтович Р.Ф. Окисление карбидов и нитридов. Киев: Наук. думка, 1981. 192 с.
 44. Gasparini C., Chater R.J., Horlait D., Vandeperre L., Lee W.E. Zirconium carbide oxidation: Kinetics and oxygen diffusion through the intermediate layer. *Journal of the American Ceramic Society*. 2018;101(6):2638–2652. <https://doi.org/10.1111/jace.15479>
 45. Kurlov A.S., Gusev A.I. Peculiarities of vacuum annealing of nanocrystalline WC powders. *International Journal of Refractory Metals and Hard Materials*. 2012;32:51–60. <https://doi.org/10.1016/j.ijrmhm.2012.01.009>

Information about the Authors





Sergey V. Briakunov – Engineer of the Laboratory of nonstoichiometric compounds of Institute of Solid State Chemistry of Ural Branch of the Russian Academy of Sciences; Senior Lecturer of Electronic Engineering Department of Ural Federal University
 **ORCID:** 0000-0002-6430-0710
 **E-mail:** s.v.briakunov@urfu.ru

Aleksey S. Kurlov – Cand. Sci. (Phys.-Math.), Head of Laboratory of nonstoichiometric compounds of Institute of Solid State Chemistry of Ural Branch of the Russian Academy of Sciences
 **ORCID:** 0000-0002-6223-4465
 **E-mail:** kurlov@ihim.uran.ru

Сведения об авторах

Сергей Владимирович Брякунов – инженер лаборатории нестехиометрических соединений, Институт химии твердого тела УрО РАН; старший преподаватель кафедры электронного машиностроения, Уральский федеральный университет
 **ORCID:** 0000-0002-6430-0710
 **E-mail:** s.v.briakunov@urfu.ru

Алексей Семенович Курлов – к.ф.-м.н., зав. лабораторией нестехиометрических соединений, Институт химии твердого тела УрО РАН
 **ORCID:** 0000-0002-6223-4465
 **E-mail:** kurlov@ihim.uran.ru

Contribution of the Authors



S. V. Briakunov – conducting the experiments, processing of the research results.
A. S. Kurlov – formation of the main concept, goal and objectives of the study, analysis of the research results, writing the text, formulation of the conclusions.

Вклад авторов

С. В. Брякунов – проведение экспериментов, обработка результатов исследований.
А. С. Курлов – формирование основной концепции, постановка цели и задачи исследования, анализ результатов исследований, подготовка текста, формулировка выводов.

Received 19.04.2022
 Revised 02.06.2022
 Accepted 06.06.2022

Статья поступила 19.04.2022 г.
 Доработана 02.06.2022 г.
 Принята к публикации 06.06.2022 г.